Long-Term Variation of the Principal Mode of Boreal Spring Hadley Circulation Linked to SST over the Indo-Pacific Warm Pool

JUAN FENG, JIANPING LI, AND FEI XIE

State Key Laboratory of Numerical Modeling for Atmospheric Sciences, and Geophysical Fluid Dynamics, Institute of Atmospheric Physics, Chinese Academy of Sciences, Beijing, China

(Manuscript received 27 January 2012, in final form 30 June 2012)

ABSTRACT

The variability of the boreal spring [March–May (MAM)] Hadley circulation (HC) is investigated, focusing on the long-term variation of the first principal mode for 1951–2008, which is an equatorially asymmetric mode (AM) with the rising branch located around 10°S. This mode explains about 70% of the variance of the MAM HC and shows an obvious upward trend and thus contributes to the strengthening of the MAM HC. The robust warming trends of sea surface temperature (SST) over the Indo-Pacific warm pool (IPWP) play an essential role in the variations of the MAM HC. When SST over the IPWP is warm, anomalous meridional circulation is induced with descending branches located in regions 30°–20°S and 5°–15°N and rising motion located near 10°S. The anomalous rising south of the equator is due to the inhomogeneous warming of SST over the IPWP. SST within the IPWP in the Southern Hemisphere shows a larger warming trend than that in the Northern Hemisphere. The position of the anomalous convergence associated with SST variations over the IPWP is aligned with the maximum meridional gradient of zonal mean SST, resulting in an equatorially asymmetric meridional circulation. This point is further established in theoretical analyses. However, the meridional SST gradient within the IPWP shows a decreasing trend, suggesting the associated anomalous meridional circulation intensifies, which in turn explains the strengthening of the MAM HC. Under this scenario, the accompanied descent in the regions of 30°–20°S and 5°–15°N is enhanced, implying a frequent drought in these regions during MAM.

1. Introduction

The Hadley circulation (HC), one of the most important atmospheric circulations, by definition, is the zonal mean meridional mass circulation in the atmosphere bounded roughly by 30°S and 30°N. The HC is thermally driven and generates an enclosed circulation in each hemisphere, with warmer air rising in the tropics and cooler air sinking in the subtropics (Held and Hou 1980). It is characterized by equatorward mass transport by the prevailing trade winds in the lower troposphere and poleward mass transport in the upper troposphere. The HC is fundamentally important to the global climate system, because its ascending and descending branches determine the climate of various tropical regions and play a role in influencing the climate at middle and high latitudes (e.g., Lindzen 1994; Chang 1995; Hou 1998). Therefore, the HC has important impacts on global climate (Diaz and Bradley 2004).

In recent years, there has been growing interest in the variations of the HC, particularly interdecadal variability. By investigating radiation, J. Y. Chen et al. (2002) showed an intensification of the HC since 1985. Similarly, Wielicki et al. (2002) suggested that the HC was intensified in the 1990s. Subsequently, the variations of the HC in the seasonal mean were discussed in many studies. Among these, the variations of the HC in boreal winter [December–February (DJF)] have been studied intensely and an obvious strengthening trend is observed. For example, Quan et al. (2004) inferred that the HC has strengthened since the 1950s by using National Centers for Environment Prediction–National Center for Atmospheric Research (NCEP–NCAR) global reanalysis data. A similar result was obtained by Quan et al. (2004), Hu et al. (2005), Mitas and Clement (2005), and Ma and Li (2008), despite different datasets or study periods used.

Corresponding author address: Dr. Jianping Li, National Key Laboratory of Atmospheric Sciences and Geophysical Fluid Dynamics (LASG), Institute of Atmospheric Physics, Chinese Academy of Sciences, P.O. Box 9804, Beijing 100029, China.
E-mail: ljp@lasg.iap.ac.cn

DOI: 10.1175/JCLI-D-12-00066.1

In the boreal summer [June–August (JJA)], previous works have found that the HC shows minor changes (e.g., Quan et al. 2004; Tanaka et al. 2004; Mitas and Clement 2006). However, there are evident weakening trends in the regional meridional circulation over 90°–150°E, 15°W–40°E, and 120°–40°W (Zhao and Moore 2008). In contrast, relatively little is known about the variability of the HC during the transition seasons: for example, boreal spring [March–May (MAM)] and autumn [September–November (SON)]. As noted by Ye and Zhu (1958) and Webster (2004), zonal wind and temperature are relatively stable with latitude during all seasons in each hemisphere, and the seasonal HC plays an important role in maintaining the balance of heat and angular momentum. Therefore, it is necessary to investigate the characteristics of the HC in different seasons.

The spatial structure of the HC has been investigated via empirical orthogonal function (EOF) analysis of the mass streamfunction (MSF), in order to explore the MSF's principal modes. Dima and Wallace (2003) showed that the annual march of the HC is dominated by two components with comparable mean-square amplitudes: one equatorially symmetric and the other equatorially asymmetric. These components vary sinusoidally with the seasonal march. Recent studies by Ma and Li (2007, 2008) have examined the year-to-year variability of the DJF HC and indicate that the principal modes of the DJF HC include an equatorially asymmetric mode and a symmetric mode, representing its decadal variability and the interannual variability, respectively. A similar result is seen in the year-to-year variability of the JJA HC (Feng et al. 2010, 2011), which is also dominated by an asymmetric mode and a quasi-symmetric mode. However, if the climatological structure of the HC is taken into account, we see that the HC is equatorially asymmetric in both DJF and JJA. To this point, one issue of interest is whether the asymmetric principal mode of the HC during DJF and JJA is dependent on the HC's climatological mean structure. If not, noting that the climatological mean structure of HC during the transition seasons is equatorial symmetric, how about the spatial features of principle modes of HC during the transition seasons? In addition, a few studies have indicated a broadening of the HC and that its poleward expansion occurs during the spring and autumn seasons in each hemisphere (e.g., Fu et al. 2006; Lu et al. 2007). A strengthening HC during boreal spring is also observed (Zhang et al. 2007). Accordingly, subtropical droughts (i.e., around 30°S and 30°N) have been more frequent in recent decades in both hemispheres during boreal spring (Hu and Fu 2007). However, these studies have not paid attention to the characteristics of principal modes of boreal spring HC, the possible causes for the formation of principal modes, or their climatic effects.

The above results suggest that further investigation of the HC variability during transition seasons is worthwhile, as it would be favorable for improving understanding of both the HC and attributes of regional climate change. In this study, we will focus on the variability of the HC during MAM, considering that the HC during MAM shows more extensive variations than those during SON as reported (Zhang et al. 2007). This provides the main motivation for this study. One of the primary goals of this work is to explore the long-term variations of the principal mode of the MAM HC, the mechanisms underlying its spatial and temporal variability, and its climatic effects. The remainder of this manuscript is divided as follows: The datasets and methodology are described in section 2. Section 3 outlines the principal mode of year-to-year variability of the MAM HC. Section 4 demonstrates the contributions of tropical SST to the variability of the MAM HC, and section 5 discusses the mechanisms of formation for the MAM HC principal mode. The potential influence of the HC on the global climate is discussed in section 6. Finally, conclusions and a discussion are presented in section 7.

2. Datasets and methodology

a. Observational datasets

The four reanalysis datasets are from NCEP–NCAR for the late 1940s–present (Kalnay et al. 1996), the NCEP–Department of Energy (DOE) Atmospheric Model Intercomparison Project (AMIP-2) covering 1979–present (Kanamitsu et al. 2002), the 40-yr European Centre for Medium-Range Weather Forecasts Re-Analysis (ERA-40) for 1957–mid-2002 (Uppala et al. 2005), and the Japanese 25-yr Reanalysis (JRA-25) for 1979–2000 (Onogi et al. 2005). All of them have a 2.5° × 2.5° horizontal resolution. Considering the period of the four reanalysis datasets, we select the span 1979–2000 as the common analysis period in which to examine the reliability of the reanalysis datasets. The principal modes and interdecadal variability of the boreal spring HC are analyzed based on NCEP–NCAR during 1951–2008 and verified by the other three reanalysis datasets. The SST data are extracted from the Improved Extended Reconstruction SST (IERSST; Smith and Reynolds 2004), which is on a 2.0° × 2.0° latitude–longitude grid, and are used to explore the influences of tropical SST on the HC. The rainfall data are from the National Oceanic and Atmospheric Administration (NOAA) precipitation reconstruction dataset (M. Chen

et al. 2002), which is on a 2.5° × 2.5° latitude–longitude grid, and are used to further establish the variation associated with the equatorially asymmetric mode (AM).

b. Methodology

The HC is characterized by the MSF of the mean meridional circulation. The MSF is obtained by vertically integrating meridional winds in the conventional way (Holton 1992; Li 2001). Clockwise circulation (the northern cell) is defined as positive and anticlockwise circulation (the southern cell) is defined as negative. The MSF is defined by

$$\psi = \int \frac{2\pi R \cos\phi}{g} [\overline{v}]\, dp, \tag{1}$$

where $[\overline{v}]$ is the zonal mean meridional wind, R is the mean radius of the earth, ϕ is the latitude, g is the gravitational acceleration, and p is the pressure. The overbar and the brackets represent temporal and zonal averaging, respectively.

The index of the MAM HC intensity (HCI) is defined as the maximum of the absolute value of the MAM MSF between 30°S and 30°N (Oort and Yienger 1996). Besides, the vertical shear of zonal mean meridional wind at 200 and 850 hPa is used to as a factor to reflect the overturning of meridional circulation, since the zonal average of the meridional wind is the same as the zonal average of the divergent meridional wind, which is often used as an index to study the HC (e.g., Song and Zhang 2007).

Singular value decomposition (SVD) analysis can be used to determine two coupled sets of orthogonal singular vectors, as well as the expansion coefficient correlations from the covariance matrix of two geophysical fields (Wallace et al. 1992; Feng and Li 2011). Here, SVD analysis is used to reveal the coupled spatial patterns between SST and mean meridional circulation (MMC) during boreal spring. Trends are computed using least squares linear regression. The relations among the MAM HC, SST, and other climatic factors are investigated by correlation and composite analyses. Here, the composite analyses for an index are the differences between the strong (greater than one positive standard deviation of the index) and weak (less than one negative standard deviation of the index) values. The EOF analysis is employed to determine the principal mode of year-to-year variability of the MAM MMC and to explore its possible contribution to the strengthening of the HC.

3. The principal mode of the variability of the boreal spring Hadley circulation

Figure 1 displays the climatological MAM MSF and its first and second principal modes determined from the NCEP–NCAR, NCEP–DOE, ERA-40, and JRA-25 datasets during the period 1979–2000. Similar features are observed in the climatological mean for all datasets (left panels in Fig. 1). The southern and northern components of the HC have equivalent magnitude and extent, with arising branch around the equator and descending branches around 30° latitude in each hemisphere.

As for the first principal mode of the MAM HC, all four datasets show an equatorially asymmetric mode dominating the variability of the MAM HC. The strong component of this mode extends from 15°S to 15°N, is centered around the equator, has a rising branch located in the Southern Hemisphere, and has a descending branch in the Northern Hemisphere. In contrast, the counterpart in the Southern Hemisphere is weak, with a descending branch positioned south of 30°S. The first principal mode of the MAM HC is similar to those during DJF (Ma and Li 2008) and JJA (Feng et al. 2011). Note that this mode is consistently observed in the four reanalysis datasets and explains about 60% of the variance of the MAM HC, indicating that this mode can be identified reliably. Moreover, the principal components (PCs) determined from each of the four datasets are highly correlated, with correlation coefficients above 0.82. The relations between HCI and the PCs from different datasets are robust (the correlation coefficients within different PCs are larger than 0.50). Besides the consistencies in the spatial structure, similar upward trends are seen in the principal components in all four datasets (Fig. 2). This result demonstrates the reliability of the enhanced equatorial asymmetric principal mode and provides confidence in employing the long-term NCEP–NCAR to illustrate the variability of the MAM HC. The second principal mode of the MAM HC is an equatorially symmetric structure. However, the variance this mode explains ranges from 19.1% (in ERA-40) to 8.7% (in JRA-25). The correlation coefficients among the second principal components from the different datasets range from 0.75 to −0.08, implying this mode is not as reliably identifiable as the first principal mode. Moreover, consider the fractional variances of the first three eigenvectors and the associated unit standard deviation of the sampling errors, which are shown in Fig. 3. According to the rule given by North et al. (1982), all of the EOF-1 modes are statistically distinguished from each other and the rest of the eigenvectors as indicated by the sampling error bars. Thus, in the following analysis we will concentrate on the equatorially asymmetric first principal mode of the MAM HC during 1951–2008 to investigate its long-term variability.

Figure 4 shows the first principal mode of the MAM HC during 1951–2008. Consistent with the result during 1979–2000, an AM is observed. This mode is similar to

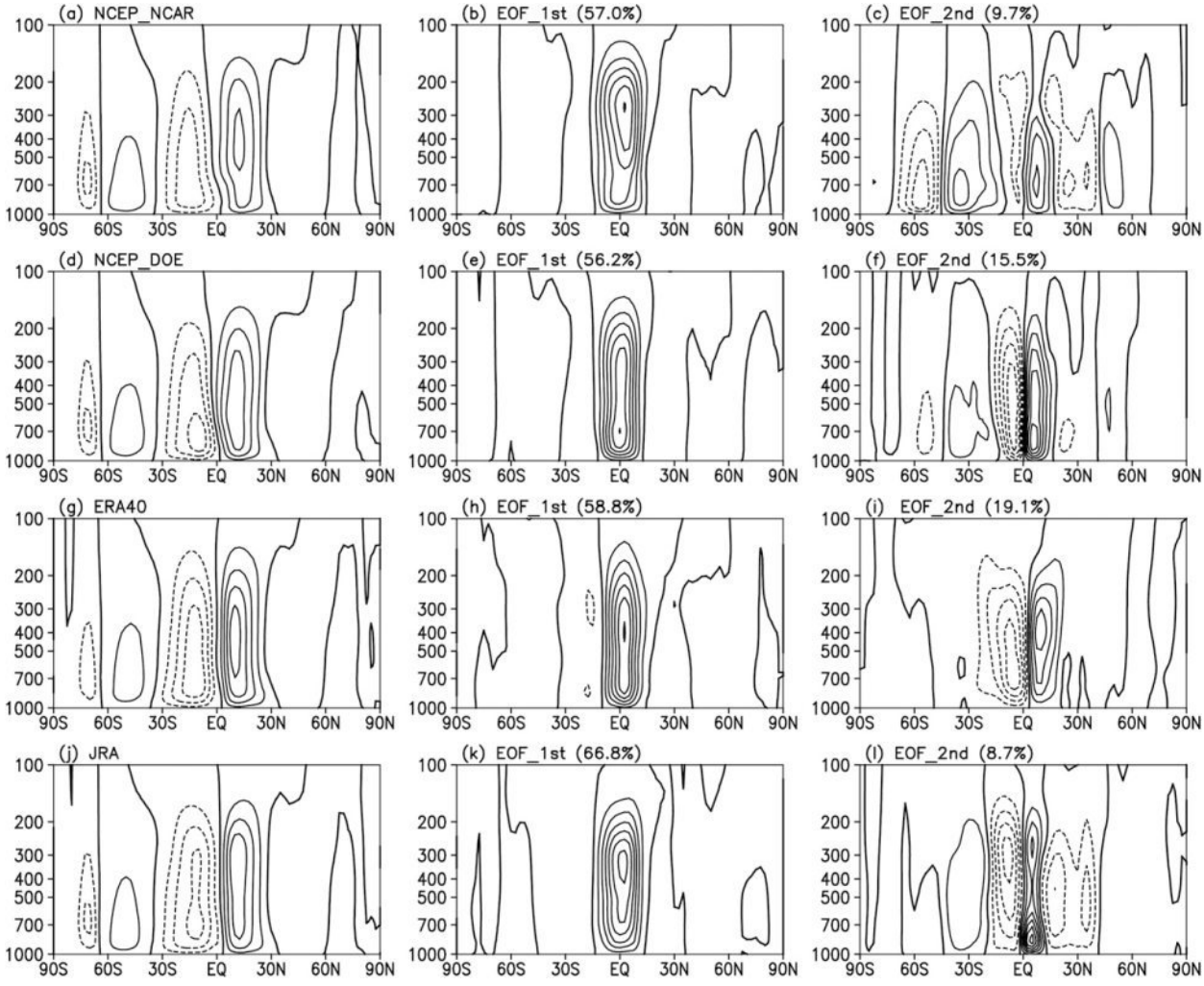

FIG. 1. (a),(d),(g),(j) The climatological mean, (b),(e),(h),(k) the first principal mode, and (c),(f),(i),(l) the second principal mode of the MAM MSF determined from (a)–(c) NCEP–NCAR, (d)–(f) NCEP/DOE, (g)–(i) ERA-40, and (j)–(l) JRA-25 over the period 1979–2000. The contour interval is 3×10^{10} kg s^{-1} in the left panels and 0.03×10^{10} kg s^{-1} in the middle and right panels. The solid (dotted) contours are positive (negative).

that in Fig. 1 but is more extensive, with the ascending branch centered near 10°S and two descending branches located south of 30°S and near 20°N. It accounts for nearly 70% of the total variance. Moreover, this mode exhibits a significant upward trend during the past six decades. For brevity, the time series of the AM is indicated by AMI in the following context. It is also seen that the AMI undergoes a decadal transformation from negative to positive values during late 1970s. That is, the phase of the AM has changed coincident with the timing of an interdecadal shift in tropical climate (e.g., Mantua et al. 1997; Xiao and Li 2007). The HCI, the strength of the MAM HC, has a clear upward trend during 1951–2008. The HCI trend is similar to the observed trend in AMI, suggesting intensification of the MAM HC may due to the variations of the AM. This point is supported by the strong correlation between the AMI and HCI (correlation coefficient of 0.81). One item of note is that the relation between the AMI and HCI is significant even if the detrended correlation is calculated, with a coefficient of 0.41. The sliding correlation (both for the raw and detrended) between the AMI and HCI with a 31-yr sliding window indicates this relationship is stable (figure not shown). This result suggests the AM contributes to the year-to-year variation of the strength of HC as well. Moreover, the trend correlation of HCI is 0.78; however, it falls to 0.28 when the effect of the AM is removed. By contrast, the trend correlation of AMI does not change much after removing the effect of HCI (coefficients vary from 0.87 to 0.65). This point further

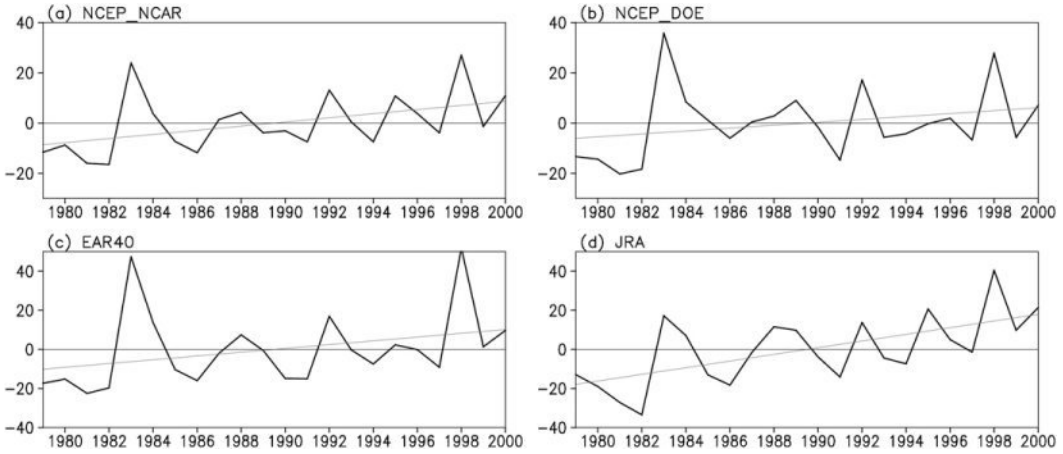

FIG. 2. Time series for the principle mode of the boreal spring Hadley circulation for the period 1979–2000. The gray sloping line is the linear trend.

supports that the strengthening of AM contribute to the strengthening of the MAM HC.

The above result indicates that as in DJF and JJA, the distinct features of the year-to-year variability of the MAM HC are dominated by an equatorially asymmetric mode. Moreover, this mode has a long-term trend of intensification, which contributes to the strengthening of the MAM HC.

4. The contribution of SST over Indo-Pacific warm pool to the variation of boreal spring Hadley circulation

The HC is a type of thermally driven circulation, and its variations are closely linked to the underlying thermal structure (Lindzen and Nigam 1987; Chiang et al. 2001; Mantsis and Clement 2009). Therefore, we examine the possible contribution of tropical SST to the intensification of the AM. SVD analysis was performed on the normalized time series during MAM of SST and MSF. The first coupled mode of normalized SST and MSF is shown in Fig. 5. We see that the most conspicuous signal is over the Indo-Pacific warm pool (IPWP; 20°S–20°N, 40°–140°E), associated with an equatorial asymmetric meridional circulation in the MSF (Fig. 5b). Moreover, the first PC of SST is closely related to the variation of SST over the IPWP (IPWPI; defined as the average of SST within 20°S–20°N, 40°–140°E and shown in Fig. 4d), with a coefficient of 0.85, and the first PC of MSF is closely linked to the HCI and AMI, with coefficients of 0.77 and 0.93, respectively. That is associated with the warming of tropical SST over IPWP an equatorial asymmetric meridional circulation is accompanied with the rising branch located around 10°S. The correlation coefficient between the corresponding expansion coefficients of the two coupled fields is 0.91, indicating variations of the AM is closely linked to the SST over IPWP.

To access the robustness of the SVD analysis, we also considered the spatial distributions of the correlation between the AMI and tropical SST and the linear trend of the MAM SST during 1951–2008 (Fig. 6). There are significant positive correlations over the IPWP, south of the eastern tropical Pacific, and in the tropical Atlantic. These areas of significant correlation are coincident with areas of significant warming trends (Fig. 6b), indicating the strengthening of the AMI is connected to the warming of tropical SST. Of note is that the warming of SST in the tropics is not equatorially symmetric with stronger signal in the Southern Hemisphere. Here, only the possible influence of SST over the IPWP on MAM HC is explored in the following context for the following considerations: 1) The IPWP is the region where the most extensive and significant SST signals are located (Figs. 5a, 6). 2) As mentioned in section 5, the AMI is significantly correlated with the meridional SST gradient

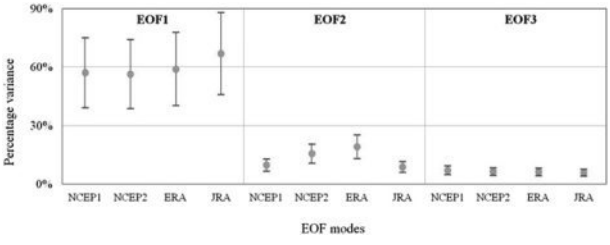

FIG. 3. Fractional variance explained by the first three EOF modes of the MAM HC based on the four reanalysis datasets for the period 1979–2000 and the associated unit standard deviation of the sampling errors.

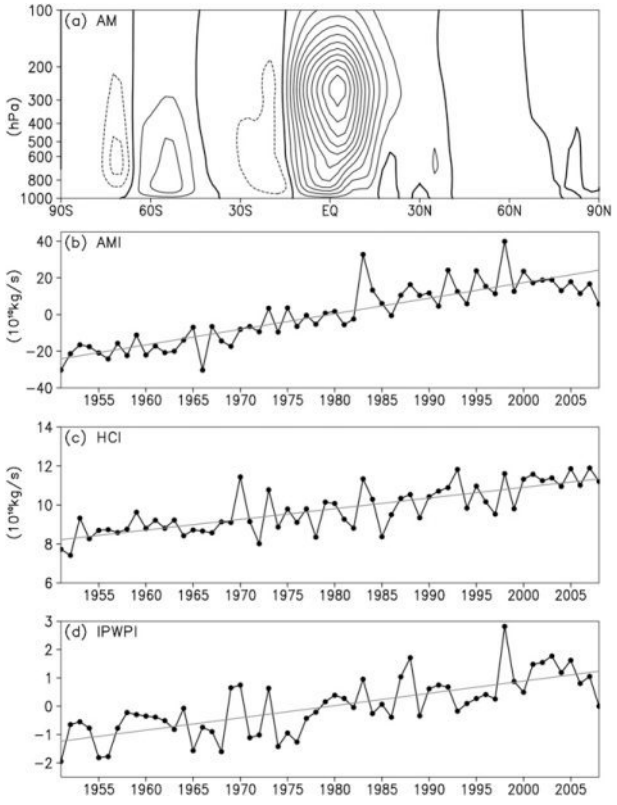

FIG. 4. (a) The principal mode of the boreal spring Hadley circulation during 1951–2008. The contour interval is 0.015×10^{10} kg s^{-1}. The solid (dotted) contours are positive (negative). (b) Time series for the principal mode of the boreal spring Hadley circulation (AMI). (c) As in (b), but for the index of the boreal spring HCI. (d) Normalized time series of SST averaged over the Indo-Pacific warm pool. The gray lines in (b)–(d) are the linear trends.

over both the IPWP and the globe with coefficients of 0.71 and 0.52, respectively. However, the correlation between AMI and meridional SST gradient over the globe turns out to be 0.32 (still significant at the 0.05 level but much smaller: i.e., 0.52 versus 0.32) when the effect of the meridional SST gradient over IPWP is removed. This result suggests the variation of AM is largely dependent on the SST variation over the IPWP. This influence of SST over the IPWP on the HC is further established by Fig. 7, which shows the anomalous meridional circulation is connected with IPWPI.

We see the warming of SST over the IPWP is accompanied by an anomalous vertical circulation, with an ascending branch near 10°S, a descending branch near 15°N, and a counterpart descending branch located to the south of 30°S. For the Southern Hemisphere, we see the variation of SST over the IPWP is associated with anomalous descent around 30°S and south (Fig. 7), overlapping the descent branch of the climatological HC (Fig. 1). This point suggests the descent branch of the southern HC is intensified. In addition, the variation of downward edge of southern cell of HC is closely linked to AMI, with a correlation of −0.46, indicating a strengthening of AM is associated with a poleward shift of the southern cell of HC. For the Northern Hemisphere, anomalous descent is seen within 10°–30°N with the maximum anomalous descent around 15°N (Fig. 7). The anomalous descent around 15°N would suppress the ascent there in the climatological circulation. Note that the magnitude of anomalous descent in the Southern Hemisphere (around 30°S) is larger than that in the Northern Hemisphere (around 30°N), which in turn implies that the broadening of Hadley circulation in the southern cell would be extensive. This point is consistent with Hu and Fu (2007) (as shown in their Fig. 3), in which they found the poleward shift of HC in the Southern Hemisphere is larger than that in the Northern Hemisphere during boreal spring. This anomalous circulation pattern is similar to that in Fig. 4a, indicating the variability of the AM is closely linked to variations of SST over the IPWP. This is further verified by the strong correlation between the AMI and the IPWPI (correlation coefficient of 0.76). Moreover, the IPWPI has a strong interdecadal variation from a negative to positive phase in the late 1970s, coincident with the timing of the AMI's phase transition, suggesting the interdecadal variations of SST over the IPWP contribute to those in the AM.

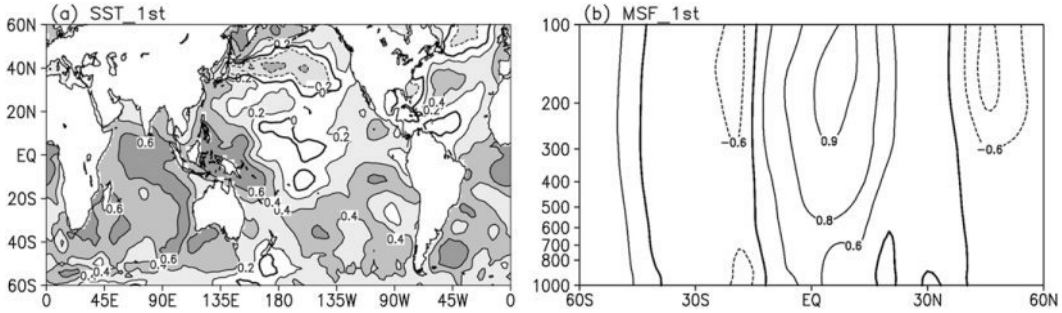

FIG. 5. (a) The heterogeneous correlation patterns for the first dominant coupled mode of the spring SST. (b) As in (a), but for the MSF.

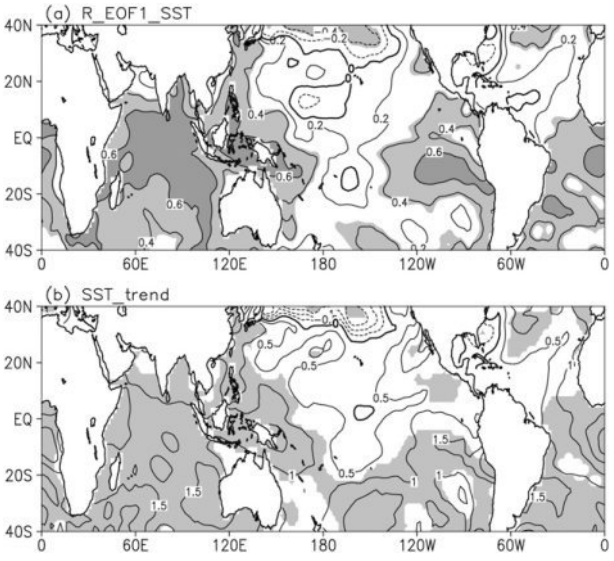

FIG. 6. (a) Spatial distribution of the correlation between the AMI and the boreal spring SST. (b) Linear trend of the boreal spring SST during 1951–2008. Shading indicates significance at the 0.05 level.

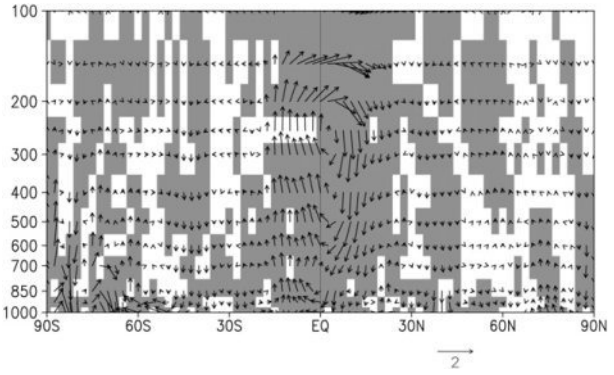

FIG. 7. Regression pattern of the meridional circulation with respect to the IPWPI. Shading indicates significance at the 0.05 level.

To provide more insight into the HC variations associated with SST over the IPWP, we further investigated spatial changes in tropospheric circulation by analyzing composite difference maps of MSF, vertical velocity, meridional wind, and the shear of meridional winds between 200 and 850 hPa for warm minus cool SST over the IPWP (Fig. 8). Here, the warm (cold) IPWP years correspond to the years that the normalized IPWPI is larger (less) than one positive (negative) standard deviation. An anomalous equatorially asymmetric meridional circulation is clearly observed in the MSF, vertical velocity, meridional wind, and shear of meridional wind. Note that the anomalous meridional circulation in Fig. 8 is similar to that shown in Fig. 4a, suggesting that the first principal mode of the MAM HC is possibly due to the SST variations over the IPWP. For example, when there is a warm event in the IPWP, anomalous ascent and convergence are seen near 10°S and are associated with anomalous descent and divergence to the south of 30°S and 20°N in each hemisphere. In addition, there are distinct differences in the meridional circulation response to warm and cool SST; the anomalous meridional circulation associated with warm SST over the IPWP is opposite to that in the case with cool SST (Fig. 8d). These anomalies associated with variations of SST over the IPWP indicate that, when the IPWP is warmer, there occurs anomalous ascent near 10°S and anomalous descent located south of 30°S and 20°N. This anomalous meridional circulation acts not only to strengthen the MAM HC but also to broaden the extent of the southern cell of MAM HC. The above result suggests the SST over the IPWP plays an essential role in modulating the variability of the MAM HC.

5. Possible cause for the formation of the MAM HC principal mode

The above analyses show that the warming of SST over the IPWP contributes to variations of the MAM HC. Of note is that the upward branch of the anomalous meridional circulation is located in the Southern Hemisphere and not near the equator or in the Northern Hemisphere as in the climatological mean. Considering that the warming of SST over the IPWP is significant between 20°S and 20°N and seems to be equatorially symmetric, it is important to investigate why the rising branch of the anomalous meridional circulation is located in the Southern Hemisphere.

To explore this issue, the time evolution of SST averaged over each hemisphere's IPWP region is shown in Fig. 9. Both the southern component (averaged over 20°S–0°, 40°–140°E) and the northern component (averaged over 0°–20°N, 40°–140°E) of SST within the IPWP exhibit significant warming trends with coefficients of 0.121° and 0.095°C decade^{-1}, respectively, from 1951 to 2008. That is, the warming within the IPWP in the Southern Hemisphere is more rapid than that in the Northern Hemisphere, as clearly indicated by their difference (Fig. 9c). Their difference (SST in 20°S–0°, 40°–140°E minus SST in 0°–20°N, 40°–140°E) shows an obvious upward trend, indicating the meridional thermal gradient within the IPWP has been suppressed in the last six decades. More rapid warming in the southern IPWP is further established in Fig. 9d, which shows the departures of zonal mean SST within the scope of IPWP from the climatological mean during the periods 1951–78 and 1981–2008. The variations of SST within 20°S–0° are much larger than those within 0°–20°N, raising the

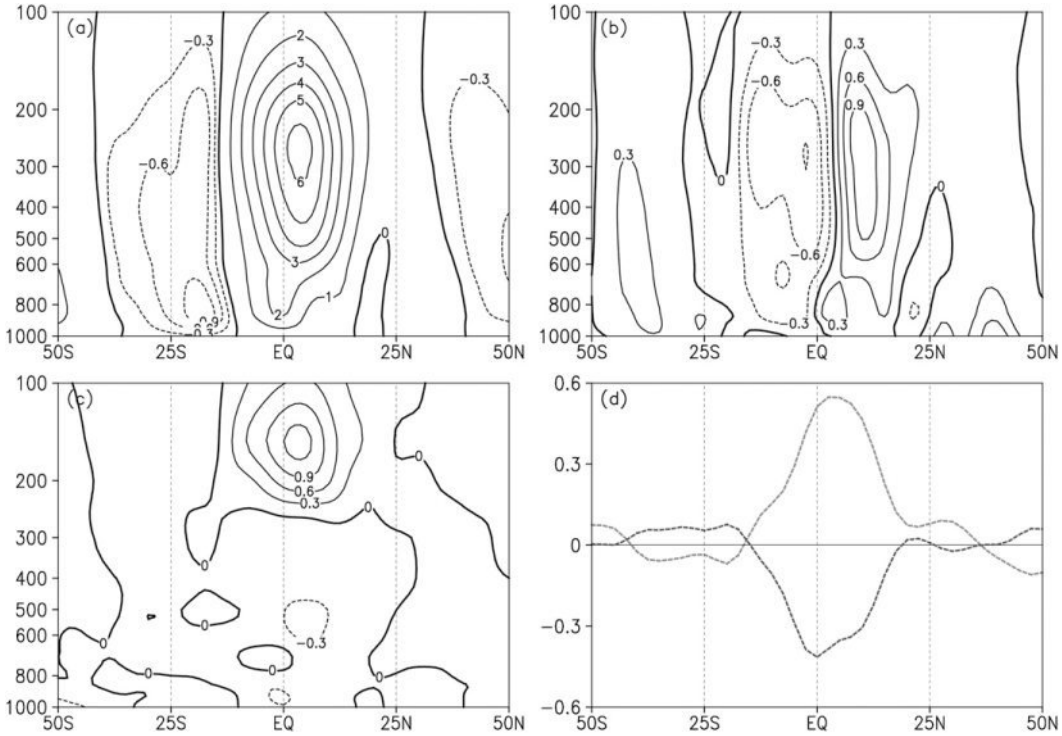

FIG. 8. Composite difference for the following properties after grouping IPWP data according to whether they are warm or cool points of SST: (a) the MSF of mean meridional circulation ($\times 10^{10}$ kg s^{-1}); the zonal means of (b) vertical velocity ($\times 10^{-2}$ Pa s^{-1}) and (c) meridional wind (m s^{-1}); and (d) the vertical shear of zonal mean meridional wind between 200 and 850 hPa for warm (gray) and cool (black) SST (m s^{-1}).

possibility that the anomalous ascent in the Southern Hemisphere may be due to the discrepancy between warming trends in the two hemispheres. This hypothesis is further examined by determining the correlations between the meridional SST gradient (SST in 20°S–0°, 40°–140°E minus SST in 0°–20°N, 40°–140°E to facilitate a direct comparison) and zonal mean vertical velocity, as shown in Fig. 10. The correlation implies an equatorially asymmetric circulation, with the main ascent located in the Southern Hemisphere and clearly seen in the meridional profile at 850 hPa. Note that the correlations in the south (~25°S) are weaker than those in the north (~15°N), which is consistent with the circulation anomalies associated with the SSTs over IPWP (Fig. 8). This result suggests the meridional circulation connected with the SST gradient is equatorially asymmetric, similar to the structure of the AM, demonstrating the meridional SST gradient within the IPWP is favorable for the formation of the AM.

Moreover, the above hypothesis is further documented by the theory proposed by Lindzen and Nigam (1987), who indicated that the SST gradient forcing is an important mechanism of the lower-level tropical flow and convergence. They obtained a steady linear model for the zonally symmetric low-level tropical flow by retaining only the zonal mean terms during the linearization of the vertically averaged momentum equations, which include the effects of back pressure. The model equations are as follows:

$$f[v] = \varepsilon[u] \quad \text{and} \tag{2}$$

$$f[u] = \left[\frac{nH_0}{2}\frac{\partial[T_s]}{\partial\varphi}\right] - \varepsilon[v], \tag{3}$$

where f is the variable Coriolis parameter; u and v are the zonal and meridional velocity, respectively; ε and n are the coefficients of turbulent friction and air expansion, respectively; brackets denote a zonal mean; H_0 is the height of the boundary layer; and T_s is the SST field. Accordingly, we can obtain the diagnostic relationship between SST and meridional wind by using (2) $\times f +$ (3) $\times \varepsilon$,

$$[v] \propto \frac{\partial[T_s]}{\partial\varphi}.$$

This relationship between SST and meridional wind indicates the meridional wind is subjected to the underlying meridional thermal gradient; that is, the positive (negative) SST meridional gradient is associated

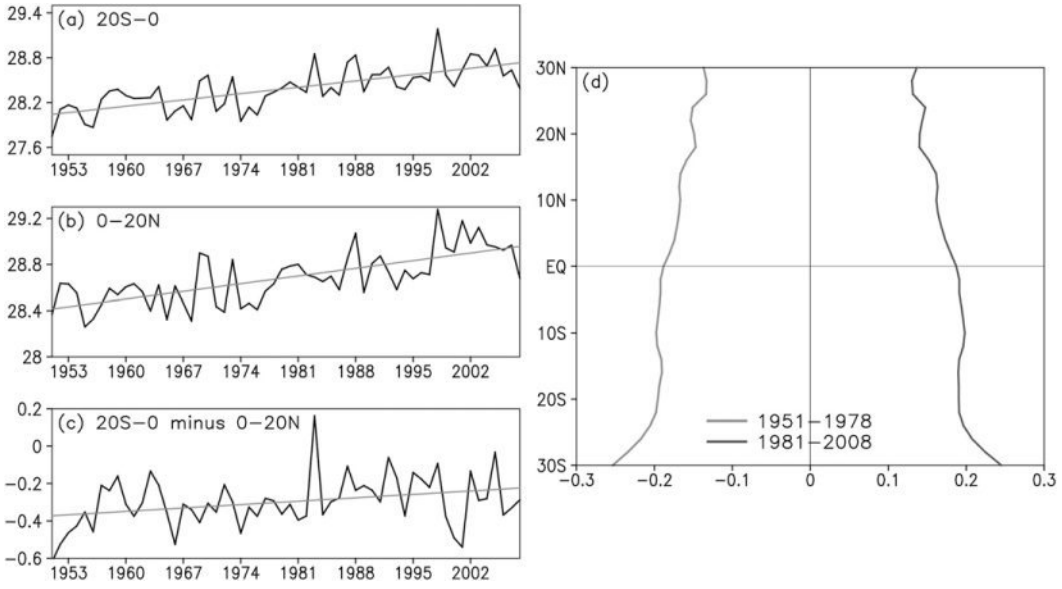

FIG. 9. Time series of SST (°C) averaged over (a) 20°S–0° and (b) 0°–20°N and (c) their difference, within 40°–140°E. (d) Profiles of SST anomaly (°C) averaged over the IPWP and two subperiods (1951–78 and 1981–2008) with respect to the climatological mean.

with southerlies (northerlies). Therefore, the position where the SST meridional gradient equals zero and varies from positive to negative corresponds to the location of convergence, which is also the location of the upward branch of the HC.

To this point, the meridional gradient of the climatological zonal mean SST is shown in Fig. 11a. To examine a smooth distribution for this gradient, a five-point smoothing has been applied according to the central difference method. The position where the gradient crosses zero is north of the equator and at the location of the ascending branch of the MAM HC shown in Fig. 1. However, if the difference between the meridional gradient of zonal mean SST anomaly for warm and cool IPWP years is examined, the position of the zero crossing is around 10°S (Fig. 11b). This point confirms the deduction above and further reveals that the position of the ascending branch of the anomalous meridional circulation associated with the IPWP's SST is due to the variations of the underlying thermal structure: that is, the inhomogeneous warming trends within the IPWP.

6. Potential influence of the variability of the MAM Hadley circulation on the global climate

Based on the discussion above, Fig. 12 shows a schematic of processes related to the influence of SST over the IPWP on the variations of the MAM HC. Under the influences of the inhomogeneous SST warming trends over the IPWP, anomalous equatorially asymmetric meridional circulation is induced. This circulation has a combined anomalous ascending branch near 10°S and two descending branches, located to the south of 30°S and approximately 15°N, respectively. The combined ascending branch is south of the climatological mean, suggesting the rate of ascent intensifies and the region

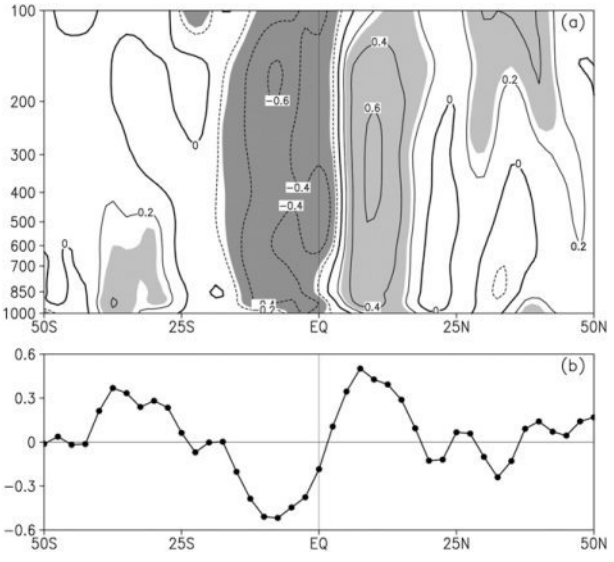

FIG. 10. (a) Distribution of correlation between the zonal mean vertical velocity and SST gradient defined as the difference in SST between 20°S–0° and 0°–20°N within the IPWP. Shading indicates significance at the 0.05 level. (b) Correlation in (a) at 850 hPa.

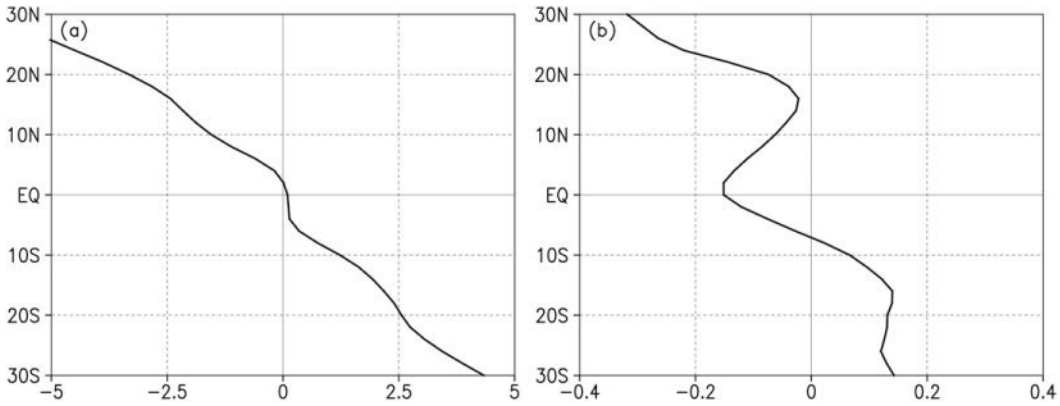

FIG. 11. (a) Meridional gradient of the climatological zonal mean SST profile. (b) Difference between the meridional gradient of zonal mean SST anomaly during warm and cool years in the IPWP.

of maximum ascent shifts southward. The descending branch of the anomalous meridional circulation in the Southern Hemisphere is superimposed on that in the climatological mean and acts to intensify the descending flow there. Meanwhile, the northern counterpart is located south of the climatological mean, suggesting descent within 5°–15°N is also enhanced. In addition, there is significant anomalous ascent around 10°S, which is also intensified.

The above deduction is further established by the spatial distribution of vertical velocity as well as its time variations (Fig. 13). The vertical velocity within 30°–20°S and 5°–15°N shows an obvious upward trend, indicating descent over these regions is enhanced. By contrast, there is a clear downward trend in velocity within 10°–5°S, implying anomalous ascent there. Note that similar trends are observed from the results based on the ERA-40, further implying the reliability of the result from the NCEP–NCAR reanalysis. Moreover, a weakening of meridional wind from 10°S to 0° is expected from the schematic. This is further verified by calculating the linear trend of zonal mean meridional wind over 10°S–0° in the lower troposphere (the average from 925 to 700 hPa), in which a significant subdued trend is observed with a coefficient of -0.29 m s^{-1} century^{-1}. The HC updraft is closely associated with convective precipitation in deep tropics and tropical precipitation is very sensitive to circulation (Chiang et al. 2002; Chiang 2004). The result raises the possibility that the MAM rainfall over regions in each hemisphere (e.g., 30°–20°S and 5°–15°N) would decrease and more frequent drought would be observed [result for the Southern Hemisphere is consistent with that in Hu and Fu (2007) and Lu et al. (2007)], while the rainfall to the south of the equator would increase. The above deduction is further supported by the long-term linear trend of boreal spring rainfall shown in Figs. 13b–d. We see the boreal spring rainfall over 30°–20°S and 5°–15°N exhibit clear decreasing trend, whereas an increasing is seen within 10°–5°S.

7. Conclusions and discussion

This study documented the long-term variability of the boreal spring HC with a focus on its spatial and temporal variations. It is found that the first predominant mode of the MAM HC is equatorially asymmetric, with the rising branch to the south of the equator. This is different from the equatorially symmetric structure in the climatological mean but is similar to the structure in the principal mode during DJF (Ma and Li 2008) and JJA (Feng et al. 2011). This result implies that the structure of the principal mode of the HC is not subjected to the HC's climatological mean structure.

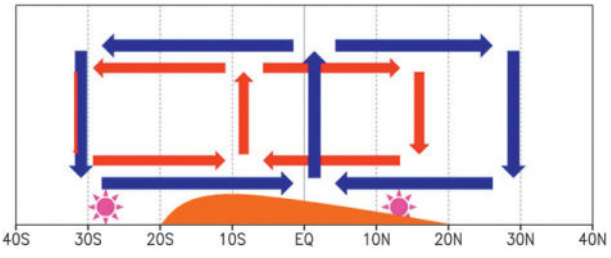

FIG. 12. Schematic diagram showing the meridional circulation anomalies associated with the inhomogeneous warming of SST over the IPWP. Blue arrows represent the climatological mean HC. Red arrows indicate the anomalous meridional circulation associated with the variations of SST over the IPWP. The orange shape between 20°S and 20°N indicates the inhomogeneous warming within the IPWP. The magenta suns indicate more frequent drought over these regions. Note that the magnitude of anomalous descent in the south takes up to about one-third compared with its northern counterpart according to Fig. 8; thus, the extent in the south is shrinking to one-third of that in the north.

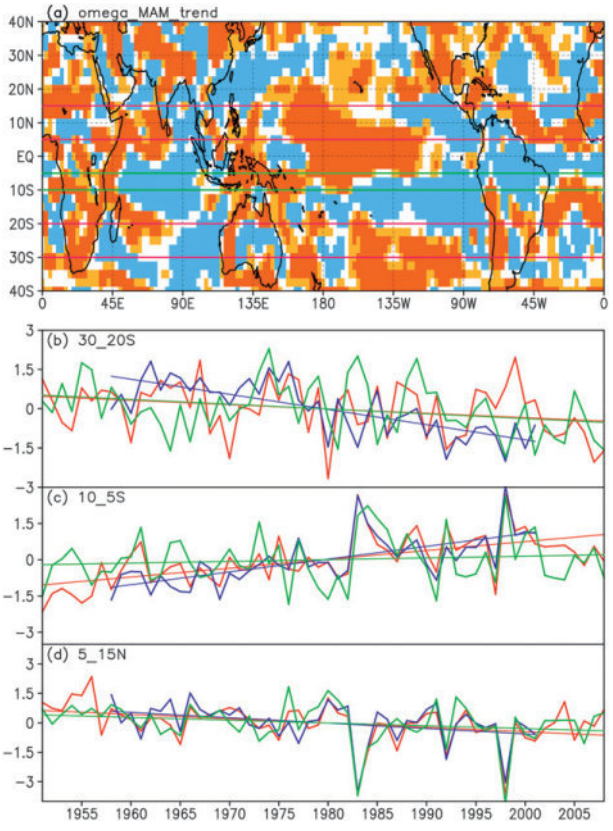

FIG. 13. (a) Linear trend of the lower-tropospheric vertical velocity averaged from 925 to 700 hPa. Red (blue) shading indicates positive (negative) values, and dark red (blue) indicates significance at the 0.2 level. Normalized time series of the zonal mean lower troposphere vertical velocity and rainfall averaged over (b) 30°–20°S, (c) 10°–5°S, and (d) 5°–15°N from 925 to 700 hPa. Thin red, blue, and green are for the result of zonal mean lower troposphere vertical velocity from NCEP–NCAR, ERA-40, and NOAA rainfall, respectively. The thin lines are the corresponding linear trends. The sign of zonal mean vertical velocity is reversed to enable a direct comparison with rainfall.

The underlying trend of warming SST over the IPWP is important in inducing variability in the MAM HC, which contributes to the intensification of the AM. The inhomogeneous warming trends within the IPWP subdue the meridional gradient of zonal mean SST and cause the rising branch of the anomalous meridional circulation to be positioned to the south of the equator. This point is further supported by the theoretical analyses. We have established that the rising in the anomalous meridional circulation is aligned with the maximum meridional gradient of zonal mean SST. Although SST has a clear warming trend over both the northern (0°–20°N) and southern (20°S–0°) IPWP during the past six decades, the trend in the southern IPWP is larger and induces an asymmetric structure in the anomalous meridional circulation. In the Southern Hemisphere, the asymmetry results in circulation that is also enhanced in the extent.

An underlying thermal structure drives the equatorially asymmetric mode in the MAM HC. Does a similar thermal structure drive an asymmetric mode in the HC during DJF and JJA? Work by Ma and Li (2008) and Feng et al. (2011) has demonstrated that SST over the IPWP plays an important role in influencing the HC in DJF and JJA, respectively. However, their work did not explain the causes of the formation of the equatorial asymmetric mode or its climatic effects. One point confirmed is that warming of SST over the IPWP surely makes an essential contribution to the HC in MAM, JJA, and DJF. SST over the IPWP during boreal autumn [September–November (SON)] also shows some warming trends that may contribute to the variability of the SON HC. In addition, only the first principal mode of the MAM HC is explored in this study, but it would be worthwhile to explore the other principal modes, as well as their variations, underlying mechanisms, and associated climatic effects.

On the other hand, the HCI used to represent the strength of MAM HC in this study is defined following the traditional notion, which is considered as the maximum absolute value of MSF within the tropics. However, this may not represent the overall behavior of the HC (i.e., both for the southern and northern cells). Considering that the southern and northern cells of MAM HC show equivalent magnitude, it is of interest to separately check the contributions of AM to the southern and northern cells. To this point, it is warranted to further investigate the long-term variation of the HC's strength for the northern and southern cells in other seasons, particularly for the boreal winter, to examine whether the reported strengthening of the boreal winter HC is seen in both the southern and the northern cell; the long-term variations of the southern and northern cell strength; and the causes of their variations, associated mechanisms, and climatic effects.

Nevertheless, we emphasized the importance of tropical SST forcing, especially SST over the IPWP, on changes in the HC. However, the SST contributions from other regions (e.g., south of the equator in the eastern Pacific and the tropical Atlantic, where significant warming is found; Fig. 6b), as well as the extratropical forcing, are not considered. Note that the phase reversal in the Pacific decadal oscillation (PDO) is roughly simultaneous with that in the AM (Hare and Mantua 2000), and SST in the eastern Pacific has a marked effect on tropical climate, as recognized. In this sense, the effects from other regions may contribute to the variability of the MAM HC, yet it is unknown to what degree they affect the MAM HC and how to quantify their relative roles. These questions remain unresolved and are worthy of future investigations.

Acknowledgments. We thank three anonymous referees, whose comments improved the paper. We wish to thank Yazhou Liu for helpful discussion. This work was jointly supported by the 973 Program (2010CB950400) and the National Natural Science Foundation of China (41205046 and 41030961).

REFERENCES

Chang, E. K. M., 1995: The influence of Hadley circulation intensity changes on extratropical climate in an idealized model. *J. Atmos. Sci.,* **52,** 2006–2024.

Chen, J. Y., B. E. Carlson, and A. D. Genio, 2002: Evidence for strengthening of the tropical general circulation in the 1990s. *Science,* **295,** 838–841.

Chen, M., P. Xie, J. E. Janowiak, and P. R. Arkin, 2002: Global land precipitation: A 50-yr monthly analysis based on gauge observations. *J. Hydrometeor.,* **3,** 249–266.

Chiang, J. C. H., 2004: Present-day climate variability in the tropical Atlantic: A model for paleoclimate changes? *The Hadley Circulation: Present, Past, and Future,* H. F. Diaz and R. S. Bradley, Eds., Kluwer Academic, 465–488.

——, S. E. Zebiak, and M. A. Cane, 2001: Relative roles of elevated heating and surface temperature gradients in driving anomalous surface winds over tropical oceans. *J. Atmos. Sci.,* **58,** 1371–1394.

——, Y. Kushnir, and A. Giannini, 2002: Deconstructing Atlantic intertropical convergence zone variability: Influence of the local cross-equatorial SST gradient and remote forcing from the eastern equatorial Pacific. *J. Geophys. Res.,* **107,** 4004, doi:10.1029/2000JD000307.

Diaz, H. F., and B. Bradley, 2004: *The Hadley Circulation: Present, Past and Future.* Kluwer Academic, 511 pp.

Dima, I. M., and J. M. Wallace, 2003: On the seasonality of the Hadley cell. *J. Atmos. Sci.,* **60,** 1522–1526.

Feng, J., and J. P. Li, 2011: Influence of El Niño Modoki on spring rainfall over south China. *J. Geophys. Res.,* **116,** D13102, doi:10.1029/2010JD015160.

Feng, R., J. P. Li, and J. C. Wang, 2010: The principal modes of variability of the boreal summer Hadley circulation and their variations (in Chinese). *Chin. J. Atmos. Sci.,* **35,** 201–216.

——, J. Li, and J. C. Wang, 2011: Regime change of the boreal summer Hadley circulation and its connection with the tropical SST. *J. Climate,* **24,** 3867–3877.

Fu, Q., C. M. Johanson, J. M. Wallace, and T. Reichler, 2006: Enhanced mid-latitude tropospheric warming in satellite measurements. *Science,* **312,** 1179, doi:10.1126/science.1125566.

Hare, S. R., and N. J. Mantua, 2000: Empirical evidence for North Pacific regime shifts in 1977 and 1989. *Prog. Oceanogr.,* **47,** 103–145.

Held, I. M., and A. Y. Hou, 1980: Nonlinear axially symmetric circulations in a nearly inviscid atmosphere. *J. Atmos. Sci.,* **37,** 515–533.

Holton, J. R., 1992: *An Introduction to Dynamic Meteorology.* 3rd ed. Academic Press, 511 pp.

Hou, A. Y., 1998: Hadley circulation as a modulator of the extratropical climate. *J. Atmos. Sci.,* **55,** 2437–2457.

Hu, Y. Y., and Q. Fu, 2007: Observed poleward expansion of the Hadley circulation since 1979. *Atmos. Chem. Phys.,* **7,** 5229–5236.

——, K.-K. Tung, and J. Liu, 2005: A closer comparison of early and late winter atmospheric trends in the Northern Hemisphere. *J. Climate,* **18,** 2924–2936.

Kalnay, E., and Coauthors, 1996: The NCEP/NCAR 40-Year Reanalysis Project. *Bull. Amer. Meteor. Soc.,* **77,** 437–471.

Kanamitsu, M., W. Ebisuzaki, J. Woollen, S.-K. Yang, J. J. Hnilo, M. Fiorino, and G. L. Potter, 2002: NCEP–DOE AMIP-II Reanalysis (R-2). *Bull. Amer. Meteor. Soc.,* **83,** 1631–1643.

Li, J. P., 2001: *Atlas of Climate of Global Atmospheric Circulation* I (in Chinese). China Meteorology Press, 279 pp.

Lindzen, R. S., 1994: Climate dynamics and global change. *Annu. Rev. Fluid Mech.,* **26,** 353–378.

——, and S. Nigam, 1987: On the role of sea surface temperature gradients in forcing low-level winds and convergence in the tropics. *J. Atmos. Sci.,* **44,** 2418–2436.

Lu, J., G. A. Vecchi, and T. Reichler, 2007: Expansion of the Hadley cell under global warming. *Geophys. Res. Lett.,* **34,** L06805, doi:10.1029/2006GL028443.

Ma, J., and J. P. Li, 2007: The reason for the strengthening of the boreal winter Hadley circulation and its connection with ENSO. *Prog. Nat. Sci.,* **17,** 1327–1333.

——, and ——, 2008: The principal modes of variability of the boreal winter Hadley cell. *Geophys. Res. Lett.,* **35,** L01808, doi:10.1029/2007GL031883.

Mantsis, D. F., and A. C. Clement, 2009: Simulated variability in the mean atmospheric meridional circulation over the 20th century. *Geophys. Res. Lett.,* **36,** L06704, doi:10.1029/2008GL036741.

Mantua, N. I., S. R. Hare, Y. Zhang, J. M. Wallace, and R. C. Francis, 1997: A Pacific interdecadal climate oscillation with impacts on salmon production. *Bull. Amer. Meteor. Soc.,* **78,** 1069–1079.

Mitas, C. M., and A. Clement, 2005: Has the Hadley cell been strengthening in recent decades? *Geophys. Res. Lett.,* **32,** L03809, doi:10.1029/2004GL021765.

——, and ——, 2006: Recent behavior of the Hadley cell and tropical thermodynamics in climate models and reanalyses. *Geophys. Res. Lett.,* **33,** L01810, doi:10.1029/2005GL024406.

North, G. R., T. L. Bell, R. F. Cahalan, and F. J. Moeng, 1982: Sampling errors in the estimation of empirical orthogonal functions. *Mon. Wea. Rev.,* **110,** 699–706.

Onogi, K., and Coauthors, 2005: JRA-25: Japanese 25-year reanalysis project—Progress and status. *Quart. J. Roy. Meteor. Soc.,* **131,** 3259–3268.

Oort, A. H., and J. J. Yienger, 1996: Observed interannual variability in the Hadley circulation and its connection to ENSO. *J. Climate,* **9,** 2751–2767.

Quan, X., H. F. Diaz, and M. P. Hoerling, 2004: Change in the Hadley circulation since 1950. *The Hadley Circulation: Present, Past, and Future,* H. F. Diaz and R. S. Bradley, Eds., Kluwer Academic, 85–120.

Smith, T. M., and R. W. Reynolds, 2004: Improved extended reconstruction of SST (1854–1997). *J. Climate,* **17,** 2466–2477.

Song, H., and M. Zhang, 2007: Changes of the boreal winter Hadley circulation in the NCEP–NCAR and ECWMF reanalyses: A comparative study. *J. Climate,* **20,** 5191–5200.

Tanaka, H. L., N. Ishizaki, and A. Kitoh, 2004: Trend and interannual variability of Walker, monsoon and Hadley circulations defined by velocity potential in the upper troposphere. *Tellus,* **56A,** 250–269.

Uppala, S. M., and Coauthors, 2005: The ERA-40 Re-Analysis. *Quart. J. Roy. Meteor. Soc.,* **612,** 2961–3012.

Wallace, J. M., C. Smith, and C. S. Bretherton, 1992: Singular value decomposition of wintertime sea surface temperature and 500-mb height anomalies. *J. Climate,* **5,** 561–576.

Webster, P. J., 2004: The elementary Hadley circulation. *The Hadley Circulation: Present, Past, and Future,* H. F. Diaz and R. S. Bradley, Eds., Kluwer Academic, 9–60.

Wielicki, B. A., and Coauthors, 2002: Evidence for large decadal variability in the tropical mean radiative energy budget. *Science,* **295,** 841–843.

Xiao, D., and J. P. Li, 2007: Spatial and temporal characteristics of the decadal abrupt changes of global atmosphere-ocean system in the 1970s. *J. Geophys. Res.,* **112,** D24S22, doi:10.1029/2007JD008956.

Ye, D. Z., and B. Z. Zhu, 1958: *Some Fundamental Problems of the General Circulation for Atmosphere* (in Chinese). Science Press, 159 pp.

Zhang, J., D. J. Gu, and N. Shi, 2007: Global mean Hadley circulation intensity index during 1948–2004 and its characteristics (in Chinese). *J. Nanning Ins. Meteor.,* **30,** 231–238.

Zhao, H. X., and G. W. K. Moore, 2008: Trends in the boreal summer regional Hadley and Walker circulations as expressed in precipitation records from Asia and Africa during the latter half of the 20th century. *Int. J. Climatol.,* **28,** 563–578.